Acta Crystallographica Section F
**Structural Biology and Crystallization Communications**
ISSN 1744-3091

# Expression, purification, crystallization and preliminary X-ray diffraction studies of triosephosphate isomerase from methicillin-resistant *Staphylococcus aureus* (MRSA252)

**Somnath Mukherjee, Debajyoti Dutta, Baisakhee Saha and Amit Kumar Das***

Department of Biotechnology, Indian Institute of Technology, Kharagpur 721302, India

Correspondence e-mail: amitk@hijli.iitkgp.ernet.in

Received 25 February 2009
Accepted 19 March 2009

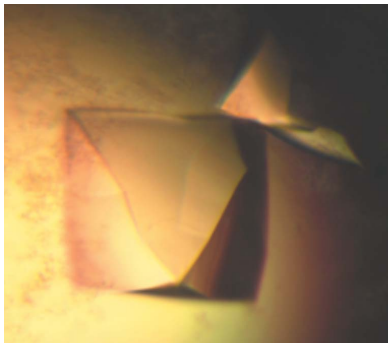



Triosephosphate isomerase from methicillin-resistant *Staphylococcus aureus* (MRSA252) was cloned in pQE30 vector, overexpressed in *Escherichia coli* M15 (pREP4) cells and purified to homogeneity. The protein was crystallized from 1.6 *M* trisodium citrate dihydrate pH 6.5 using the hanging-drop vapour-diffusion method. The crystals belonged to space group $P4_32_12$, with unit-cell parameters $a = b = 79.15$, $c = 174.27$ Å. X-ray diffraction data were collected and processed to a maximum resolution of 1.9 Å. The presence of two molecules in the asymmetric unit gave a Matthews coefficient ($V_M$) of 2.64 Å$^3$ Da$^{-1}$, with a solvent content of 53.63%.

## 1. Introduction

The conversion of glucose to pyruvate in the glycolytic pathway results in the generation of ATP, which meets the primary energy demands of the cell. Among the enzymes of the glycolytic pathway, triosephosphate isomerase (TPI, TIM, D-glyceraldehyde-3-phosphate ketol-isomerase; EC 5.3.1.1), a ubiquitous enzyme, catalyzes interconversion between the ketose–aldose isomers dihydroxyacetone phosphate (DHAP) and glyceraldehyde-3-phosphate (GAP) (Rieder & Rose, 1959; Rose, 1962). TPI is known as an 'evolutionary perfect enzyme' since its high catalytic capacity is a diffusion-limited process. The catalytic mechanism involves binding of the substrate DHAP, abstraction of the proton at C1 of the substrate by a general base, yielding the *cis*-enediolate intermediate, and finally protonation of the enediolate species at C2 by a general acid to yield the product GAP. The conserved active-site glutamate is recognized as the general base responsible for proton capture at C1 of the substrate DHAP or, in the reverse reaction, of the proton at C2 of GAP. An important role is played by histidine, which shuttles a proton between the two O atoms of the enediolate intermediates (Fig. 1). Thus, 'if a single message emerges after all the mechanistic and structural scrutiny of TIM, it is one of precision' (Knowles, 1991). In the absence of enzyme, this is a very energetically unfavourable reaction owing to the high p$K_a$ of the C1 atom of the substrate. In the enzymatic environment several residues contribute to facilitating this step, in particular those that stabilize the negative charge on the O atom of the adjacent carbonyl group (Kursula & Wierenga, 2003). A number of three-dimensional structures of TIMs from various prokaryotes and from unicellular as well as higher eukaryotes have been reported to date. The classic $\beta_8\alpha_8$ fold, also known as the 'TIM barrel', emerged from these crystal structures. The TIM barrel comprises eight repeats of strand–turn–helix–turn units, forming a parallel eight-stranded $\beta$-barrel surrounded by eight $\alpha$-helices on the outside of the molecule. The active-site loop of TIM (also called the flexible loop, the lid loop or loop 6) comprises about ten residues. This loop has been suggested to move as a rigid body that 'breathes on hinges' between two well defined conformations. These conformations, termed 'open' and 'closed', have been described in detail (Lolis *et al.*, 1990; Lolis & Petsko, 1990; Joseph *et al.*, 1990; Davenport *et al.*, 1991; Wierenga *et al.*, 1991; Wierenga, Borchert *et al.*, 1992; Wierenga, Noble *et al.*, 1992). The loop holds the substrate in place and protects the enediol intermediate from being hydrolyzed. This hinged-lid motion is an intrinsic property of the enzyme and the nature of the

ligands affects the relative populations of the conformers. In most TIMs reported to date, a dimeric state of the enzyme is physiologically active. Extensive studies of the enzyme kinetics, reaction mechanism and structures of TIM from different sources have resulted in a considerable body of currently available knowledge on structure–function relationships in this enzyme (Aparicio *et al.*, 2003).

*Staphylococcus aureus* is one of the most dreaded opportunistic nosocomial human pathogens and is responsible for minor skin infections to life-threatening diseases such as meningitis, pneumonia, osteomyelitis, endocarditis, septic arthritis, toxic shock syndrome and septicaemia (Archer, 1998). The resistance of this bug to antibiotics such as methicillin and vancomycin has further added to its already growing menace. The methicillin-resistant *S. aureus* MRSA252 possesses a single triosephosphate isomerase (SaTIM; SAR0830) comprised of 253 amino acids. SaTIM is one of the components of the cell-envelope proteins from this pathogen (Gatlin *et al.*, 2006) and is involved in biofilm formation. TIM was identified as one of five genes that were upregulated during biofilm formation, which may be a consequence of oxygen limitation in the deeper layers of the biofilm (Becker *et al.*, 2001). It has also been shown that glycolytic enzymes that are located on the cell surface possess additional properties. In *S. aureus*, a surface-associated transferrin-binding protein was identified as the glycolytic enzyme glyceraldehyde-3-phosphate dehydrogenase (Modun & Williams, 1999). Thus, it can be argued that during biofilm formation the upregulation of glycolytic enzymes is stimulated by factors other than oxygen limitation in the cell, which may reflect their putative role in complex microbial population and reduced antimicrobial susceptibility. Being responsible for the production of ATP in glycolysis, this enzyme also serves as a very good target for drug design against the glycolytic pathway. Therefore, we have focused our attention on structural and mechanistic studies of this important enzyme. The present work reports the cloning, overexpression, purification, crystallization and preliminary X-ray diffraction studies of SaTIM from MRSA252.

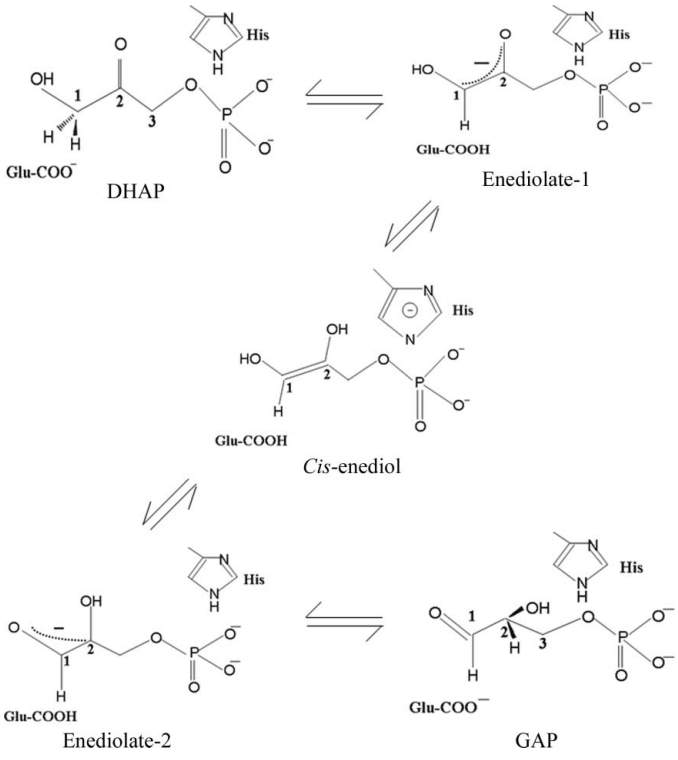


**Figure 1**
Mechanistic outline of the interconversion between DHAP and GAP by TIM.

## 2. Materials and methods

### 2.1. Cloning

The sequences corresponding to the open reading frame of SaTIM were amplified by PCR using the MRSA252 genomic DNA as the template with the primer pair 5′-CGGGATCCATGAGAACACCAATTATAGCTGG-3′ (forward primer with a *Bam*HI recognition site) and 5′-GCCCCAAGCTTTTATTTTGCACCTTCTAAC-3′ (reverse primer with a *Hin*dIII recognition site). The purified PCR product was cloned into the *Bam*HI and *Hin*dIII sites of the expression vector pQE30 (Qiagen, USA), which adds six consecutive histidines to the immediate upstream of multiple cloning sites. The recombinant DNA was then transformed into *E. coli* M15 (pREP4) cells and subsequently selected on ampicillin/kanamycin plates. The positive clones were verified by DNA sequencing. As no intervening residues were introduced between the six consecutive histidines and the start codon of SaTIM for proteolytic cleavage of the N-terminal tag in subsequent steps, the desired construct has HHHHHHM at its N-terminus.

### 2.2. Overexpression and purification

The positive clone harbouring the desired construct of SaTIM was grown in Luria broth with 100 µg ml$^{-1}$ ampicillin and 25 µg ml$^{-1}$ kanamycin at 310 K for 3 h, during which the $A_{600}$ reached 0.6, induced with 100 µ*M* IPTG and grown for a further 5 h at 310 K to maximize the overexpression of the recombinant protein in the cytosolic fraction. The cells from 1 l culture were resuspended in buffer *A* (10 m*M* Tris–HCl pH 8.0, 300 m*M* NaCl and 10 m*M* imidazole) containing 0.1 m*M* each of leupeptin, pepstatin and aprotinin and 0.02 m*M* phenylmethylsulfonyl fluoride (PMSF). The suspension was lysed by ultrasonication on ice and the lysate was centrifuged at 22 000*g* for 40 min. The supernatant was loaded onto Ni-Sepharose High Performance affinity matrix (GE Healthcare Biosciences) pre-equilibrated with buffer *A*. The column was then washed extensively with buffer *A* followed by buffer *B* (10 m*M* Tris–HCl pH 8.0, 300 m*M* NaCl and 50 m*M* imidazole) to remove bound contaminants. The protein was finally eluted with buffer *C* (10 m*M* Tris–HCl pH 8.0, 300 m*M* NaCl and 300 m*M* imidazole). The eluted protein was subjected to size-exclusion chromatography using Superdex 75 prep-grade matrix in a 16/70C column (GE Healthcare Biosciences) on an ÄKTAprime Plus system (GE Healthcare Biosciences) equilibrated with buffer *D* (10 m*M* Tris–HCl pH 8.0, 50 m*M* NaCl, 2 m*M* DTT). 2 ml fractions were collected at a flow rate of 1 ml min$^{-1}$. The fractions containing the desired protein were pooled together. The protein concentration was estimated by the method of Bradford (1976) and the purity was verified by 15% SDS–PAGE.

### 2.3. Crystallization

The purified protein was concentrated to 80 mg ml$^{-1}$ using a 10 kDa cutoff Vivaspin 20 concentrator (GE Healthcare). 2 µl droplets of protein solution in buffer *D* were mixed with an equal volume of reservoir solution and equilibrated against 1 ml of the latter using commercially available sparse-matrix screens from Hampton Research (Crystal Screen and Crystal Screen II) at 298 K and the hanging-drop vapour-diffusion method in 24-well Linbro plates. Prismatic crystals appeared from 1.6 *M* trisodium citrate dihydrate pH 6.5 after 3 d at 298 K.

### 2.4. Data collection

The diffraction data were collected at our home source equipped with a Rigaku R-AXIS IV$^{++}$ detector using Cu $K\alpha$ X-rays generated by a Rigaku Micromax HF007 Microfocus rotating-anode X-ray generator with a Varimax mirror system and operated at 40 kV and 30 mA (Rigaku Americas Corporation). The reservoir solution was used as the cryoprotectant and the crystals were flash-cooled in a liquid-nitrogen stream at 100 K using a Rigaku X-stream 2000 cryosystem. The crystals diffracted to a maximum resolution of 1.9 Å. Data were collected over a range of 180° with an oscillation angle of 0.5°. A total of 360 frames were collected with an exposure time of 2 min per frame and a crystal-to-detector distance of 123 mm. Diffraction data were processed with *d*TREK* v.9.8 software (Pflugrath, 1999).

## 3. Results and discussion

SaTIM was successfully cloned and purified to homogeneity with an N-terminal $His_6$ tag. The molecular weight of monomeric $His_6$-TIM, 28.5 kDa, as predicted from the sequence, was confirmed by 15% SDS–PAGE (Fig. 2). A typical crystal measured 1.5 × 1.3 × 0.9 mm (Fig. 3). Diffraction data were collected using a single crystal at 100 K. The crystals diffracted to a maximum of 1.9 Å resolution.

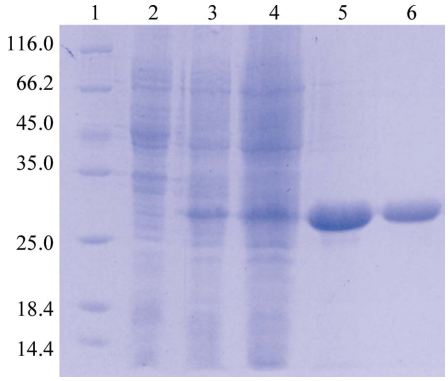


**Figure 2**
15% SDS–PAGE analysis. Lane 1, molecular-weight markers (kDa); lane 2, uninduced M15 cells; lane 3, induced M15 cells; lane 4, supernatant; lane 5, SaTIM after Ni–NTA chromatography; lane 6, purified SaTIM after size-exclusion chromatography.

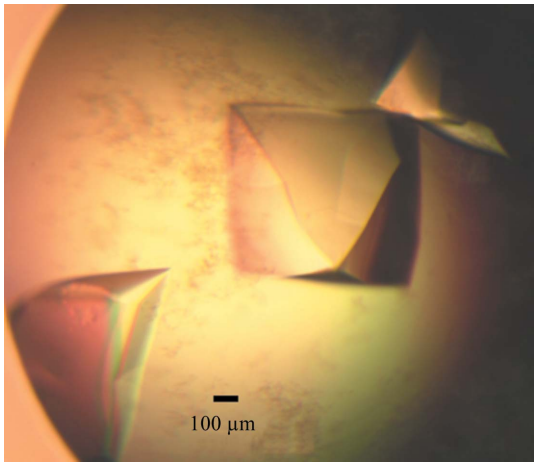


**Figure 3**
Crystals of SaTIM: a typical crystal of SaTIM grown from 1.6 *M* trisodium citrate dihydrate pH 6.5 at 298 K measured 1.5 × 1.3 × 0.9 mm.

**Table 1**
Data-collection and processing statistics.

Values in parentheses are for the highest resolution shell.

| | |
|---|---|
| Wavelength (Å) | 1.54 |
| Space group | $P4_32_12$ |
| Unit-cell parameters | |
| $a = b$ (Å) | 79.15 |
| $c$ (Å) | 174.27 |
| Unit-cell volume (Å$^3$) | 1098131.75 |
| Matthews coefficient (Å$^3$ Da$^{-1}$) | 2.64 |
| Solvent content (%) | 53.63 |
| No. of molecules in ASU | 2 |
| Resolution range (Å) | 26.16–1.90 (1.97–1.90) |
| Observed reflections | 538712 |
| Unique reflections | 83952 |
| Redundancy | 6.42 (6.85) |
| Completeness (%) | 99.9 (100.0) |
| $R_{merge}$† (%) | 7.2 (42.9) |
| Average $I/\sigma(I)$ | 9.5 (2.9) |

† $R_{merge} = \sum_{hkl}\sum_i |I_i(hkl) - \langle I(hkl)\rangle| / \sum_{hkl}\sum_i I_i(hkl)$, where $I_i(hkl)$ is the observed intensity of a reflection and $\langle I(hkl)\rangle$ is the mean of reflection $hkl$.

Analysis of symmetry and the systematic absences in the recorded diffraction patterns indicated that the crystals belonged to the tetragonal $P4_12_12/P4_32_12$ space group, with unit-cell parameters $a = b = 79.15$, $c = 174.27$ Å. The Matthews coefficient suggested the presence of two molecules in the asymmetric unit, with 53.63% solvent content ($V_M$ = 2.64 Å$^3$ Da$^{-1}$; Matthews, 1968). A total of 538 712 observed reflections were merged to 83 952 unique reflections in the 26.16–1.9 Å resolution range. The overall completeness of the data set was 99.9%, with an $R_{merge}$ of 7.2%. The data-collection and processing statistics are given in Table 1. Using the program *BLASTP* 2.2.20+ (Altschul *et al.*, 1997, 2005), it was found that SaTPI has a high sequence identity of 57% to its nearest homologue, TPI from *Geobacillus stearothermophilus* (PDB code 2btm; Alvarez *et al.*, 1999). Thus, the molecular-replacement method was used to solve the structure using the *MOLREP* program (Vagin & Teplyakov, 1997) within the *CCP*4 package (Collaborative Computational Project, Number 4, 1994) with 2btm as the search model. Since the Matthews coefficient suggested the presence of two molecules in the asymmetric unit, the number of monomers was set to two in the search parameters while running *MOLREP*. A promising solution with a homodimeric structure and interpretable electron density was only obtained (correlation coefficient of 0.53) for space group $P4_32_12$. Thus, the space group of SaTIM was unambiguously ascertained as $P4_32_12$. The model was subsequently subjected to rigid-body refinement in *REFMAC*5 (Murshudov *et al.*, 1997) within the *CCP*4 package, giving an $R$ factor of 44%. Final model building and restrained refinement using *REFMAC*5 are currently in progress. In parallel with the refinement, we are preparing crystals of SaTIM complexed with substrate analogues in order to study their mode of interaction.

This work was carried out with financial assistance from the Department of Biotechnology, Government of India. SM thanks the Council of Scientific and Industrial Research, Government of India for an individual fellowship. We thank Dr S. Panjikar, EMBL, Hamburg for his kind help and suggestions.

## References

Altschul, S. F., Madden, T. L., Schäffer, A. A., Zhang, J., Zhang, Z., Miller, W. & Lipman, D. J. (1997). *Nucleic Acids Res.* **25**, 3389–3402.
Altschul, S. F., Wootton, J. C., Gertz, E. M., Agarwala, R., Morgulis, A., Schäffer, A. A. & Yu, Y. K. (2005). *FEBS J.* **272**, 5101–5109.

Alvarez, M., Wouters, J., Maes, D., Mainfroid, V., Rentier-Delrue, F., Wynes, L., Depiereux, E. & Martial, J. A. (1999). *J. Biol. Chem.* **274**, 19181–19187.
Aparicio, R., Ferreira, S. T. & Polikarpov, I. (2003). *J. Mol. Biol.* **334**, 1023–1041.
Archer, G. L. (1998). *Clin. Infect. Dis.* **26**, 1179–1181.
Becker, P., Hufnagle, W., Peters, G. & Herrmann, M. (2001). *Appl. Environ. Microbiol.* **67**, 2958–2965.
Bradford, M. M. (1976). *Anal. Biochem.* **72**, 248–254.
Collaborative Computational Project, Number 4 (1994). *Acta Cryst.* D**50**, 760–763.
Davenport, R. C., Bash, P. A., Seaton, B. A., Karplus, M., Petsko, G. A. & Ringe, D. (1991). *Biochemistry*, **30**, 5821–5826.
Gatlin, C. L., Pieper, R., Huang, S. T., Mongodin, E., Gebregeorgis, E., Parmar, P. P., Clark, D. J., Alami, H., Papazisi, L., Fleischmann, R. D., Gill, S. R. & Peterson, S. N. (2006). *Proteomics*, **6**, 1530–1549.
Joseph, D., Petsko, G. A. & Karplus, M. (1990). *Science*, **249**, 1425–1428.
Knowles, J. R. (1991). *Nature (London)*, **350**, 121–124.
Kursula, I. & Wierenga, R. K. (2003). *J. Biol. Chem.* **278**, 9544–9551.
Lolis, E., Alber, T., Davenport, R. C., Rose, D., Hartman, F. C. & Petsko, G. A. (1990). *Biochemistry*, **29**, 6609–6618.
Lolis, E. & Petsko, G. A. (1990). *Biochemistry*, **29**, 6619–6625.
Matthews, B. W. (1968). *J. Mol. Biol.* **33**, 491–497.
Modun, B. & Williams, P. (1999). *Infect. Immun.* **67**, 1086–1092.
Murshudov, G. N., Vagin, A. A. & Dodson, E. J. (1997). *Acta Cryst.* D**53**, 240–255.
Pflugrath, J. W. (1999). *Acta Cryst.* D**55**, 1718–1725.
Rieder, S. V. & Rose, I. A. (1959). *J. Biol. Chem.* **234**, 1007–1010.
Rose, I. A. (1962). *Brookhaven Symp. Biol.* **15**, 293–309.
Vagin, A. & Teplyakov, A. (1997). *J. Appl. Cryst.* **30**, 1022–1025.
Wierenga, R. K., Borchert, T. V. & Noble, M. E. (1992). *FEBS Lett.* **307**, 34–39.
Wierenga, R. K., Noble, M. E. & Davenport, R. C. (1992). *J. Mol. Biol.* **224**, 1115–1126.
Wierenga, R. K., Noble, M. E., Postma, J. P., Groendijk, H., Kalk, K. H., Hol, W. G. J. & Opperdoes, F. R. (1991). *Proteins*, **10**, 33–49.